

Cinnabarinic acid provides hepatoprotection against non-alcoholic fatty liver disease

Nikhil Y. Patil¹, Iulia Rus¹, Emma Downing¹, Ashok Mandala², Jacob E. Friedman²,
Aditya D. Joshi^{1,2*}

¹Department of Pharmaceutical Sciences, University of Oklahoma Health Sciences
Center, Oklahoma City, OK 73117

²Harold Hamm Diabetes Center, University of Oklahoma Health Sciences Center,
Oklahoma City, OK 73117

Running Title: Cinnabarinic acid protects against NAFLD

Corresponding Author: * Dr. Aditya D. Joshi, Department of Pharmaceutical Sciences, University of Oklahoma Health Sciences Center, 1110 N. Stonewall Ave., Oklahoma City, Oklahoma 73117, E-mail: aditya-joshi@ouhsc.edu

Number of Pages: 42

Number of Tables: 0

Number of Figures: 9

Number of References: 66

Abstract word count: 229

Introduction word count: 640

Discussion word count: 1475

Abbreviations: AhR, aryl hydrocarbon receptor; ALT, alanine aminotransferase; Arnt, AhR nuclear translocator; BSA, bovine serum albumin; CA, cinnabarinic acid; CD, control diet; FBS, fetal bovine serum; FFA, free fatty acids; HCC, hepatocellular carcinoma; HFD, high-fat diet; NAFLD, Nonalcoholic fatty liver disease; NASH, non-alcoholic steatohepatitis; OA, oleic acid; PA, palmitic acid; PBS, phosphate-buffered saline; Stc2, stanniocalcin 2; TCDD, dioxin, 2,3,7,8-tetrachlorodibenzo-p-dioxin; TG, triglycerides; XRE, xenobiotic response element

Recommended Section: Gastrointestinal, Hepatic, Pulmonary, and Renal

ABSTRACT

Nonalcoholic fatty liver disease (NAFLD) is a chronic condition in which excess lipids accumulate in the liver and can lead to a range of progressive liver disorders including non-alcoholic steatohepatitis, liver cirrhosis, and hepatocellular carcinoma. While lifestyle and diet modifications have proven to be effective as NAFLD treatments, they are not sustainable in long-term and currently no pharmacological therapies are approved to treat NAFLD. Our previous studies demonstrated that cinnabarinic acid (CA), a novel endogenous Aryl hydrocarbon Receptor (AhR) agonist activates AhR target gene, Stanniocalcin 2 and confers cytoprotection against a plethora of ER/oxidative stressors. In this study, the hepatoprotective and anti-steatotic properties of CA were examined against free fatty acid-induced *in vitro* and high-fat diet-fed *in vivo* NAFLD models. The results demonstrated that CA treatment significantly lowered weight gain and attenuated hepatic lipotoxicity both before and after established fatty liver, thereby protecting against steatosis, inflammation and liver injury. CA mitigated intracellular free fatty acid uptake concomitant with the downregulation of CD36/fatty acid translocase. Genes involved in fatty acid and triglyceride synthesis were also downregulated in response to CA treatment. Additionally, suppressing AhR and Stc2 expression using RNA interference *in vitro* verified that the hepatoprotective effects of CA were absolutely dependent on both AhR and its target, Stc2. Collectively, our results demonstrate that endogenous AhR agonist, CA confers hepatoprotection against NAFLD by regulating hepatic fatty acid uptake and lipogenesis.

SIGNIFICANCE STATEMENT

In this study using *in vitro* and *in vivo* models, we demonstrate that cinnabarinic acid (CA), an endogenous AhR agonist provides protection against non-alcoholic fatty liver disease. CA bestows cytoprotection against steatosis and liver injury by controlling expression of several key genes associated with lipid metabolism pathways, limiting the hepatic lipid uptake, and controlling liver inflammation. Moreover, CA-induced hepatoprotection is absolutely dependent on the AhR and Stc2 expression.

INTRODUCTION

Nonalcoholic fatty liver disease (NAFLD), distinguished by profuse acquisition of triglycerides in the liver is the most prevalent chronic liver disease world-wide (Le et al., 2021). NAFLD is often linked with obesity, type 2 diabetes, atherosclerosis, and cardiovascular diseases, increasing the risk of mortality (Angulo, 2002; Cohen et al., 2011; Wójcik-Cichy et al., 2018). The pathology of NAFLD can progress from hepatic steatosis to non-alcoholic steatohepatitis (NASH; steatosis with inflammation and fibrosis), to cirrhosis, hepatocellular carcinoma (HCC), and ultimately organ failure (Bugianesi et al., 2002; Cobbina and Akhlaghi, 2017; de Alwis and Day, 2008; Farrell and Larter, 2006; White et al., 2012). The mechanisms for the progression of NAFLD are complex and a multiple parallel hit hypothesis has been proposed to underlie the pathogenesis, which is not completely understood (Friedman et al., 2018). The onset of fatty liver disease is attributed to imbalance in hepatic lipid homeostasis due to elevated uptake of hepatic fat, increased *de novo* lipogenesis, reduced fat oxidation and lipid export (Ipsen et al., 2018; Postic and Girard, 2008). Furthermore, excessive accumulation of lipids in hepatocytes can trigger oxidative stress, inflammation, apoptosis, and fibrosis, sequentially or simultaneously leading to the progression of the disease (Day and James, 1998; Tilg and Moschen, 2010).

The ubiquitously expressed ligand-dependent transcription factor Aryl hydrocarbon Receptor (AhR) is known to play a role in xenobiotic metabolism and liver homeostasis (Mimura and Fujii-Kuriyama, 2003; Mitchell et al., 2006; Park et al., 2005; Savouret et al., 2003; Wu et al., 2007; Zhou et al., 2010). In the canonical pathway, ligand binding results in conformational changes and nuclear translocation of AhR,

followed by dimerization of AhR with AhR nuclear translocator (Arnt) and binding to the xenobiotic response elements (XREs, GCGTG motif) present in the promoter region of AhR regulated genes (Denison and Nagy, 2003; Probst et al., 1993; Reyes et al., 1992; Wright et al., 2017). 2,3,7,8-tetrachlorodibenzo-p-dioxin (TCDD) is a prototypical exogenous AhR agonist of anthropic origin that is known to activate plethora of detoxification genes, including cytochrome P450 1A1 (encoded by Cyp1a1) (Ma et al., 2009; Ma, 2001; Nebert et al., 1993) . Recent studies examining the role of AhR in fatty acid metabolism and NAFLD reported that TCDD-induced AhR activation resulted in hepatic steatosis and fibrosis (Lee et al., 2010; Nault et al., 2016; Zhu et al., 2020). On the other hand, treatment with endogenous AhR agonists indole and indole-3 acetic acid attenuated steatosis (Hendrikx and Schnabl, 2019; Ji et al., 2019). We recently identified a tryptophan metabolite cinnabarinic acid (CA) as an endogenous activator of AhR that failed to induce hepatic Cyp1a1 but upregulated a novel AhR target gene, stanniocalcin 2 (Stc2) in the liver. Stc2 is a glycosylated peptide hormone involved in development, calcium regulation, angiogenesis, cell apoptosis, and proliferation (Joshi, 2020). CA treatment conferred protection against ethanol-induced liver steatosis, injury and hepatocyte apoptosis in both acute and chronic models of alcoholic liver injury. However, its role in fatty acid or dietary high fat diet – induced lipotoxicity has not been studied previously.

In the current study we interrogated the ability of the novel AhR ligand CA to protect specifically against palmitic and oleic acid-induced *in vitro* and high-fat diet (HFD) – fed *in vivo* NAFLD models, and identified potential molecular and metabolic pathways conferring the protection. Our data strongly suggest that CA treatment

significantly reduced fatty acid deposition in oleic and palmitic acid treated HepG2 and AML12 cells. In a high-fat diet-fed NAFLD model, CA administration reduced weight gain, alleviated hepatic steatosis, metabolic deterioration, liver triglyceride and cholesterol content, and mitigated liver injury. Moreover, CA treatment limited hepatic lipid uptake and fatty acid synthesis by downregulating expression of genes involved in fatty acid uptake, de novo lipogenesis, and triglyceride synthesis. Finally, the present study provides compelling evidence that the anti-steatotic properties exerted by CA are uniquely dependent upon AhR activated Stc2 signaling.

MATERIALS AND METHODS

Cell culture and *in vitro* treatments. HepG2 (ATCC, HB-8065), the human hepatocellular carcinoma cell line, was grown in MEM medium (ThermoFisher Scientific, Waltham, MA) containing 10% fetal bovine serum (FBS) (R&D Biosystems, Minneapolis, MN) and 1% 100x penicillin-streptomycin solution (ThermoFisher Scientific), whereas differentiated non-transformed mouse hepatic cells – AML12 (ATCC, CRL-2254) were cultured in DMEM:F12 medium (ThermoFisher Scientific) supplemented with 10% FBS, 1% 100x ITS (ThermoFisher Scientific) containing insulin, transferrin, and selenium, 40 ng/ml dexamethasone (Millipore Sigma, St. Louis, MO), and 1% 100x penicillin-streptomycin solution. Cells were maintained in a humidified 5% CO₂ incubator at 37°C. Cells were treated with 500 μM BSA (Cayman Chemical, Ann Arbor, MI) + DMSO (control); 30 μM CA (CA-only) for 24 hrs.; 500 μM BSA-palmitate saturated fatty acid complex (palmitic acid, PA) or 500 μM BSA-oleate monounsaturated fatty acid complex (oleic acid, OA) for 24 hrs. (PA or OA-only); 30 μM CA and 500 μM PA or OA simultaneously for 24 hrs. (CA+PA or CA+OA); and 500 μM PA or OA for 24 hrs. followed by 30 μM CA treatment for additional 24 hrs. (CA after PA or CA after OA). For *in vitro* knockdown studies, HepG2 cells were transfected with 50 nM Dharmacon SMARTpool ON-TARGETplus AhR siRNA, Stc2 siRNA and Non-targeting siRNAs (NT siRNA) (Horizon Discovery, Boyertown, PA) for 24 hrs. using DharmaFECT 4 transfection reagent according to the manufacturer's instructions. Cells were further treated with control, CA-only, PA or OA-only, CA+PA or CA+OA, and CA after PA or CA after OA.

Animals and *in vivo* treatments. Eight-week-old female C57BL/6J mice (wild type, WT) (Jackson Laboratory, Bar Harbor, ME) were used in accordance with the guidelines of the Institutional Animal Care and Use Committee at the University of Oklahoma Health Sciences Center. Mice were housed in plastic cages with corn cob bedding in a climate and temperature-controlled facility. One week after adaptation, mice were fed normal control diet (CD) (D12450J) or high-fat diet (HFD) (D12492) (Research Diet, New Brunswick, NJ) and randomly assigned to 4 groups (7 mice in each group): 1) CD, mice fed with control diet (10 kcal% fat) for 16 weeks; 2) HFD, mice on a high fat diet (60 kcal% fat) for 16 weeks; 3) CA+HFD, mice fed with high-fat diet and treated with CA for 16 weeks; and 4) CA after HFD, mice fed with high-fat diet for 16 weeks with CA treatment initiated after 10 weeks of exposure to HFD for remaining 6 weeks. The Organic Chemistry Core (University of Texas Medical Branch, Galveston) synthesized and provided CA for the experiments. Mice received 12 mg/kg (body weight) CA thrice a week on Monday, Wednesday and Fridays via intraperitoneal (i.p.) injections. Both food and water were provided *ad libitum*. Mice weight and food intake were measured weekly for 16 weeks, after which mice were euthanized by overdose of isoflurane followed by removal of vital organ as a secondary confirmation method. Blood samples were collected and livers were excised and weighed.

Cell viability assay. To measure the effect of free fatty acids on cell viability, 2×10^4 cells were plated in a 96 well culture plate and treated with different concentrations (0 μ M, 100 μ M, 250 μ M, 500 μ M, 750 μ M, 1000 μ M) of OA or PA for 24 hrs. Cell viability was measured using the RealTime-Glo™ MT Cell Viability Assay (Promega, Madison, WI) following the manufacturer's protocol.

Oil red O Staining. Cells were seeded on Laboratory-Tek II chamber slides at 80% confluency as described earlier (Guo et al., 2020). Cells were washed with PBS, incubated in propylene glycol for 5 minutes, and incubated overnight in oil red O solution (abcam, Waltham, MA). Stained slides were further treated with 85% propylene glycol for 1 minute and rinsed twice with distilled water. The slides were then incubated in hematoxylin solution for 1-2 minutes to counterstain the nuclei, rinsed thoroughly with tap water and two changes of distilled water. Cells were imaged with Nikon ECLIPSE Ni epifluorescence microscope (Nikon, Melville, NY). Quantitation of lipid droplets was performed using ImageJ. Additionally, a colorimetric assay was performed to quantify the oil red O accumulation. Cells grown and treated in a 6-well plate were washed with PBS and 400 μ l isopropanol was added to each well to dissolve the oil red O. From each well, 100 μ l aliquots were transferred to a 96-well plate and absorbance was measured at 500 nm on a Synergy 2 plate reader (Agilent, Santa Clara, CA).

Histological examination. To observe the pathological changes, liver tissues were kept in 10% neutral buffered formalin and submitted to the Stephenson Cancer Center Tissue Pathology Core (University of Oklahoma Health Sciences Center) for paraffin embedding, sectioning and H&E staining.

Measurement of lipid content. Triglycerides (TG) from cultured cell lysates, and liver tissue homogenates were measured using the Triglyceride-Glo™ Assay (Promega, Madison, WI). Cholesterol from the liver tissue samples was detected using the Cholesterol/Cholesterol Ester-Glo™ Assay (Promega). Intracellular fatty acid quantification in HepG2 and AML12 cells was performed using fluorometric free fatty acid assay kit (abcam). To determine fatty acid uptake, a QBT fatty acid uptake kit

(Molecular Devices, San Jose, CA) was utilized. All the assays were performed as per manufacturer's instructions and fluorescence/luminescence measured using Synergy 2 microplate reader (Agilent).

Glucose tolerance Test. Mice were fasted for 6 hrs. before receiving an oral bolus of 2 gm of glucose (Sigma-Aldrich) per kilogram of body weight. Blood glucose measurements were performed using Accu-check Guide Me meter (Roche, Indianapolis, IN) on blood samples taken from the tail vein at 0, 15, 30, 60, 90 and 120 min.

Alanine aminotransferase assay. The ALT activity kit (abcam) was used according to the manufacturer's protocol to fluorometrically measure the serum alanine aminotransferase (ALT).

RNA isolation and quantitative real time – polymerase chain reaction (qRT-PCR).

Total RNA was extracted from liver tissues or treated HepG2 and AML12 cells using TRIzol™ reagent (ThermoFisher Scientific) and quantified. The iScript™ cDNA Synthesis Kit (Bio-Rad, Hercules, CA) was used to synthesize first-strand cDNA from 1 µg total RNA. Quantitative RT-PCR was performed using gene-specific primers (IDT, Coralville, IA) (Supp. Table 1) and PowerUp SYBR Green Master Mix (ThermoFisher Scientific) on a StepOnePlus real time PCR system (ThermoFisher Scientific). The relative expression level of each sample was expressed as fold change using 18S ribosomal RNA as a reference gene.

Western blot Analysis. Whole tissue lysates were fractionated by SDS-PAGE electrophoresis (Bio-Rad) and transferred to low fluorescence PVDF membranes using Trans-Blot Turbo system (Bio-Rad). Membranes were probed using AhR (Enzo

Lifesciences, Farmingdale, NY), and Stc2 (ProSci Inc, Poway, CA) (Joshi et al., 2022) antibodies. Proteins were detected using fluorescently labeled secondary antibodies (Bio-Rad) followed by imaging using the ChemiDoc MP imaging system (Bio-Rad).

Chromatin Immunoprecipitation. Liver tissue extracted from mice were fixed with 1% formaldehyde and subjected to chromatin-immunoprecipitation (ChIP) using the ChIP-IT Express Enzymatic Kit (Active Motif) as described previously (2022). The protein-bound DNA complexes were immunoprecipitated using antibodies against AhR (abcam, Cambridge, MA), IgG (negative control) (abcam), and histone H3 (positive control) (Cell Signaling Technology, Danvers, MA). Primers specific to the Cyp1a1 and Stc2 promoters (Supp. Table 2) were used to PCR amplify the input and immunoprecipitated DNA. PCR products electrophoresed on 5% polyacrylamide gel and stained with SYBR green (ThermoFisher Scientific) were imaged using the ChemiDoc MP imaging system (Bio-Rad).

Statistical Analysis. Both *in vitro* and *in vivo* experiments performed - including animal/sample size, data acquisition methods and data analysis protocols were preset for this hypothesis-testing study (Michel et al., 2020). Animal numbers required was determined based on our previous observations and using G*Power statistical suite ($\alpha = 0.05$ and $\beta = 0.80$) (Faul et al., 2009). CA and free fatty acid treatments were performed using appropriate blinding methods and controls. Data were analyzed by applying multivariate ANOVA models, unless noted in the figure legends, using Sigma Plot software (Systat Software, San Jose, CA). After the overall significant F test from the mixed-effects multivariate ANOVA model, the post hoc multiple comparison tests were performed for the prespecified comparisons adjusted by the Tukey procedure. All

results are expressed as the means \pm standard deviations (SD). Differences between the groups were considered significant only if the P value was <0.05 .

RESULTS

CA attenuates steatosis in PA/OA-treated HepG2 and AML12 cells. To determine an optimal concentration of free fatty acids that mimic *in vitro* model of NAFLD without inducing overt cytotoxicity, a cell viability assay was performed in HepG2 and AML12 cells with varying concentrations of PA and OA. We observed that both PA and OA significantly decreased cell viability in HepG2 cells at concentrations higher than 500 μ M (Fig. 1A). Whereas, in AML12 cells, significant cytotoxicity was observed at 750 μ M (Fig. S1A). Consequently, all subsequent *in vitro* experiments in HepG2 and AML12 cells were performed using 500 μ M PA and OA concentrations. Our previous study has determined activation of AhR – as reflected by maximal induction of AhR target gene, Stc2 – with 30 μ M CA treatment for 24 hr (Joshi et al., 2015). Here, we examined CA's capability to protect against PA/OA induced steatosis in both HepG2 and AML12 cells. Oil red O staining indicated significant accumulation of lipids in both cell lines with 500 μ M free fatty acid treatment, thus validating the *in vitro* NAFLD model used in the study (Fig. 1B and C). Simultaneous treatment of CA with PA/OA as well as CA administration 24 hrs. after PA/OA treatment showed significant reduction in steatosis both in HepG2 (Fig. 1B and C) and AML12 (Fig. S1B and C) cells compared with PA/OA-only treatment. Colorimetric oil red O measurement assay corroborated aforementioned findings and confirmed that CA attenuated PA/OA induced lipid accumulation in both HepG2 (Fig. 1D) and AML12 (Fig. S1D) cells.

CA decreases intracellular lipid accumulation in PA/OA-treated *in vitro* model of NAFLD. An increase in uptake of free fatty acids by hepatocytes and *de novo* lipogenesis are known to stimulate excess accumulation of intracellular triglycerides that

causes hepatic steatosis and lipotoxicity (Kawano and Cohen, 2013). Therefore, we first measured accumulation of total intracellular triglyceride and free fatty acid content in presence of PA/OA-only as well as with CA treatment. Simultaneous as well as post-treatment with CA significantly alleviated triglyceride and free fatty acid content in HepG2 (Fig. 2A and B) and AML12 (Fig. S2A and B) cells. Concurrent CA treatment, CA + PA and CA + OA reduced triglyceride levels by 53-65% and 51-66% whereas CA treatment after PA/OA decreased cellular triglycerides by 35-43% and 37-47% in HepG2 and AML12 cells respectively. Similarly, free fatty acid content in HepG2 and AML12 cells was reduced with CA treatment (Fig. 2B and Fig S2B). Overall, simultaneous CA and PA/OA treatment resulted in greater reduction in triglyceride and free fatty acid content compared with CA administration 24-hr after free fatty acid treatment. In order to understand effect of CA treatment on the mobility of long-chain fatty acids, an intracellular uptake of fluorescently labeled fatty acid analog, BODIPY-dodecanoic acid was measured. CA treatment attenuated uptake of free fatty acids in both HepG2 (Fig. 2C) and AML12 (Fig. S2C) cells.

Downregulation of genes involved in free fatty acid uptake, lipid metabolism and inflammation with CA treatment. To investigate the mechanism by which CA bestows its anti-steatotic effects, changes in the gene expression profiles of several key genes involved in lipid metabolism pathways were measured. Quantitative RT-PCR indicated upregulation of the fatty acid translocase CD36 in PA/OA-only treated cells which was significantly reduced upon CA treatment (Fig. 3A and S3A). Expression of genes involved in fatty acid synthesis, including acetyl-CoA carboxylase 1 (ACC1), fatty acid synthase (FASN), stearoyl-CoA desaturase 1 (SCD1), sterol regulatory element binding

protein-1 (SREBP1), peroxisome proliferator-activated receptor gamma (PPAR γ), and perilipin 2 (PLIN2) were increased with PA/OA treatments (Fig. 3B and S3B). CA treatment attenuated expression of aforementioned genes involved in lipogenesis (Fig. 3B and S3B). Both concurrent and post-treatment with CA significantly decreased the mRNA message of glycerol-3-phosphate acyltransferase 1 mitochondrial (GPAM), glycerol-3-phosphate acyltransferase 2 (GPAT2), diacyl glycerol acyl transferase 2 (DGAT2), and monoacylglycerol O-acyltransferase 1 (MOGAT1) that are associated with triglyceride synthesis (Fig. 3C and S3C). Simultaneous CA and PA/OA treatment as well as CA treatment after PA administration also reduced expression of diacyl glycerol acyl transferase 1 (DGAT1), a critical enzyme responsible for the conversion of diacylglycerols to triglycerides (Fig. 3C and S3C). Expression of markers of inflammation and pro-inflammatory cytokines including, tumor necrosis factor alpha (TNF α), transforming growth factor beta (TGF β), monocyte chemoattractant protein (MCP1), and monocyte-macrophage marker F4/80 were suppressed in response to CA treatment (Fig. 3D and S3D). Our results thus highlight role of CA in averting the NAFLD pathology in an *in vitro* model by reducing the uptake, synthesis, and deposition of lipids, and curbing the inflammatory responses.

CA treatment reduces body mass gain in high-fat diet fed mice. We next evaluated CA's potential to protect against an *in vivo* high-fat diet induced model of non-alcoholic fatty liver disease. Mice were fed with the control diet (CD); high-fat diet (HFD); HFD with CA administration for 16 weeks (CA + HFD); and HFD for 16 weeks with CA-regimen starting from week 10 (CA after HFD). As expected, the HFD-fed mice gained significantly higher body mass than CD-fed mice. Treatment with CA reduced the weight

gain in both CA + HFD and CA after HFD groups (Fig. 4A-C). Mice in CA + HFD group displayed significant loss of weight gain after 9 weeks of CA treatment. The body mass gain of mice in the CA after HFD group was similar to that of the HFD group until week 9, but started to decline after CA administration from week 10 with significant reduction in body mass from week 14 (Fig. 4B-C). The liver weight and liver weight normalized to total body weight was reduced significantly in CA-treated mice (Fig. 4D-E). Finally, the reduction in weight gain upon CA treatment was not attributed to the caloric consumption as there were no differences in dietary intake between various groups (Fig. 4F).

CA alleviates steatosis and hepatic injury as well as improves glucose metabolism. Long-term high-fat diet feeding is known to induce metabolic disturbances and macrovascular steatosis. Therefore, we examined role of CA in regulating hepatic lipid deposition. Histopathological analysis revealed that HFD-fed mice developed severe steatosis compared to the CD-fed mice, while treatment with CA mitigated the lipid accumulation in liver (Fig. 5A). Moreover, CA regimen resulted in the reduction of hepatic triglyceride and cholesterol content (Fig. 5B-C). Serum ALT assays confirmed that the liver injury induced by the high-fat diet was attenuated with CA treatment (Fig. 5D). These data confirmed that CA exerts anti-steatotic and cytoprotective effects against high fat diet induced lipotoxicity. Hepatic steatosis is connected with impaired glucose metabolism, therefore we measured blood glucose levels and conducted an oral glucose tolerance test (Ochi et al., 2017). CA treatment significantly lowered the fasting blood glucose levels (Fig. 6A) and improved glucose tolerance (Fig. 6B-C) indicating recuperation from metabolic deterioration.

CA regulates lipid metabolism *in vivo*. In order to obtain mechanistic insight by which CA mitigates hepatic lipid accumulation several key genes regulating fatty acid uptake and metabolism were examined. Both CA + HFD and CA after HFD treatments resulted in the significant downregulation of CD36 - which facilitates hepatic uptake of long-chain fatty acids (Fig. 7A). Correspondingly, several critical genes regulating lipid synthesis that were upregulated under HFD-fed conditions, showed significant decrease after CA treatment (Fig. 7B-C). Treatment with CA significantly upregulated liver mRNA levels of mitochondrial beta oxidation genes, carnitine palmitoyl transferase 1a (CPT1a) and carnitine palmitoyl transferase 2 (CPT2). However, no change in the expression of acyl-CoA oxidase1 (ACOX1), a marker of peroxisomal oxidation was seen (Fig. 7D). CA administration mitigated inflammatory response as observed by the downregulation of the expression of the inflammatory markers (Fig. 7E). Collectively, our data suggests that CA treatment regulates free fatty uptake and attenuates *de novo* lipogenesis thereby ameliorating steatosis observed in NAFLD.

CA-induced steatoprotection is dependent on AhR-driven Stc2 signaling. CA is a known AhR agonist that specifically induce hepatic expression of an AhR target gene, Stc2 without Cyp1a1 upregulation (Patil et al., 2022). In HFD-fed mice livers, Stc2 expression was downregulated (Fig. S4A). Upon CA treatment, AhR directly interacted with the Stc2 promoter region containing 8 XRE's resulting in a significant induction of Stc2 without Cyp1a1 upregulation (Fig. S4A and C) (Harper et al., 2013; Joshi et al., 2015). Moreover, CA treatment resulted in Stc2 upregulation *in vitro*, indicating activation of an AhR signaling cascade (Fig. S4B). Knowing that the CA-induced AhR-mediated Stc2 expression is critical for the protection against plethora of endoplasmic

reticulum/oxidative stressors (Joshi et al., 2015), we investigated whether the anti-steatotic effects of CA are mediated by AhR-Stc2 signaling. First, the role of AhR in CA-mediated protection was interrogated by silencing AhR in HepG2 cells. HepG2 cells were transiently transfected with AhR siRNA and non-targeting (scrambled) oligonucleotides. AhR expression was suppressed with RNA interference and confirmed by Western blotting (Fig. 8A). Using histology, we analyzed the degree of steatosis in AhR-silenced OA-treated HepG2 cells in the presence and absence of CA. CA-treatment failed to provide protection against OA-induced steatosis in AhR knocked-down cells, whereas in AhR-positive cells (non-targeting siRNA treated) - CA markedly attenuated accumulation of intracellular lipids (Fig. 8B). Subsequent quantitation of triglycerides and free fatty acids in AhR-silenced PA/OA- treated HepG2 cells indicated no effect of CA treatment (Fig. 8C-D). In contrast, control HepG2 cells treated with CA reduced both triglycerides and free fatty acid content (Fig. 2A-B). Suppressing AhR in HepG2 cells elevated long-chain fatty acid uptake compared to untransfected (control) and nontargeting siRNA treated cells. CA treatment did not attenuate free fatty acid uptake in AhR silenced HepG2 cells, but was able to mitigate fatty acid uptake in control and nontargeting siRNA treated cells (Fig. 8E). We further investigated if silencing AhR in HepG2 cells had any effect on the expression of genes associated with lipid metabolism and inflammation when induced with PA/OA and treated simultaneously or after 24 hrs. with CA. In the absence of AhR, CA treatment did not downregulate genes involved in fatty acid uptake (CD36), fatty acid synthesis (ACCA1, FASN, SREBP1, PPAR γ), triglyceride synthesis (GPAM, GPAT2, DGAT1, DGAT2, MOGAT1), and inflammation (TNF α , TGF β , MCP1, F4/80) (Fig. 8 F-I). To further interrogate potential

function of AhR target gene, *Stc2* in CA-induced AhR-driven protection against lipotoxicity – *Stc2* expression in HepG2 cells was knocked-down using RNA interference (Fig. 9A). In the absence of *Stc2*, CA did not protect against steatosis (Fig. 9B), or mitigated triglyceride, fatty acid accumulation, and hepatic uptake of free fatty acids (Fig. 9C-E). Moreover, in *Stc2* silenced cells, CA treatment failed to attenuate expression of fatty acid uptake, lipid synthesis, and inflammation markers (Fig. 9F-I). Therefore, the findings presented here strongly indicate that the anti-steatotic and hepatoprotective effects against lipotoxicity exerted by CA are absolutely dependent upon AhR-mediated *Stc2* signaling.

DISCUSSION

Non-alcoholic fatty liver disease is a liver manifestation of metabolic syndrome in the absence of alcohol intake. It covers an array of pathological conditions ranging from steatosis to complex hepatocellular injury, inflammation, and fibrosis (non-alcoholic steatohepatitis, NASH). The global epidemic of NAFLD, the number one hepatic disease worldwide is rapidly increasing owing to growing prevalence of obesity and type 2 diabetes mellitus. In the United States, NAFLD is affecting around 85 million adults and 8 million children, and currently is a second most common cause of liver transplantation (Shetty and Syn, 2019). Currently, lifestyle changes by diet and exercise are shown to be most effective interventions against NAFLD (Fernández et al., 2022). Additionally, American Association for the Study of Liver Diseases guidelines recommend use of off-label piaglitazone, a PPAR γ agonist and vitamin E for biopsy proven NASH adult patients only after discussing and considering risks and benefits (Zhang and Yang, 2021). With absence of Food and Drug Administration approved treatments, characterization of unmined pathways and identification of novel future therapeutics is warranted.

Cinnabarinic acid, a tryptophan metabolite and a byproduct of kynurenine pathway is shown to be an endogenous agonist for AhR (Lowe et al., 2014). Taking advantage of cre-lox system to manipulate status of AhR, our previous study identified Stc2 as a novel receptor target gene (Harper et al., 2013). These findings were important as CA treatment induced expression of Stc2 in an AhR-dependent manner, and failed to upregulate expression of archetypical AhR target gene, Cyp1a1 in liver

(Joshi et al., 2015). Very few studies have investigated the therapeutic potential of CA. CA protected against endoplasmic reticulum/oxidative stress induced apoptosis in isolated primary hepatocytes (Joshi et al., 2015). Moreover, CA conferred protection against steatosis, apoptosis, and hepatic injury in an acute and NIAAA chronic plus binge model of alcoholic liver disease, in an AhR and Stc2 dependent manner (Joshi et al., 2022; Joshi et al., 2015). In an experimental model of multiple sclerosis in mice, daily CA injections (0.1 – 10 mg/kg) protected against autoimmune encephalomyelitis (Fazio et al., 2014). In mice, basal concentration of CA is \approx 400 pg/ml and \approx 10 pg/mg in serum and liver respectively. A daily 12 mg/kg CA i.p. regimen elevated CA concentration in serum to \approx 6000 pg/ml and resulted in 50% increase in a liver CA concentration (\approx 15 pg/mg) (Joshi et al., 2022). Our *in vivo* studies have observed activation of AhR and upregulation of Stc2 within 2 hr of 12 mg/kg CA treatment (Patil et al., 2022), and a daily CA administration was able to maintain an elevated Stc2 expression (Fig. S4A and C) (Joshi et al., 2022). These observations indicate that from a clinically relevant therapeutic perspective, a pharmacotherapeutic formulation or dietary supplementation of CA will be essential for activating AhR-Stc2 mediated hepatoprotective signaling pathways. A recent study indicated half-life of CA to be 4 hr in an isolated rat liver microsomes (Gómez-Piñeiro et al., 2022), therefore future studies will need to be performed to comprehensively examine mechanism of CA production within endogenous tryptophan metabolism pathway, and determine *in vivo* stability of CA.

Selection and specificity of AhR agonists, ligand-induced conformational changes in AhR recruiting various enhancing/inhibitory cofactors, specific post-translational

modifications responsible for promoter modulation, and subsequent signaling pathways contribute towards the potential detrimental or beneficial function of AhR in NAFLD (Carambia and Schuran, 2021; Murray and Perdew, 2020; Safe et al., 2018). TCDD regimen resulted in an AhR mediated upregulation of the fibrogenic pathway and development of liver fibrosis (Pierre et al., 2014). An activation of AhR with Benzo[a]pyrene promoted fatty liver disease (Zhu et al., 2020), whereas administration of AhR antagonist, α -naphthoflavone attenuated hallmarks of NAFLD (Xia et al., 2019). Therefore, in response to various exogenous ligands, AhR has been implicated to promote NAFLD by regulating expression of target genes including CD36, CYP1A1, TNF- α , Fibroblast growth factor 21 (FGF21) (Lee et al., 2010; Walisser et al., 2005; Xia et al., 2019; Zhu et al., 2020). On the contrary, a protective role of AhR in NAFLD has also been documented. Loss of AhR has shown to cause multiple physiological abnormalities including accelerated rate of apoptosis, decreased liver size and liver fibrosis around portal triad (Fernandez-Salguero et al., 1995). Recently, a hepatocyte-specific AhR knockout mouse model indicated AhR's protective role against high-fat diet induced hepatic steatosis and lipotoxicity by regulation of Socs3 gene (Wada et al., 2016). A gut-microbiota derived tryptophan metabolite mitigated fatty acid induced inflammation and lipogenesis in hepatocytes – and the effects were AhR-dependent (Krishnan et al., 2018). Similarly, microbiota derived endogenous AhR ligands indole-3-acetic acid and indole were able to attenuate steatosis in NAFLD (Hendrikx and Schnabl, 2019; Ji et al., 2019). CA unlike prototypical AhR agonists does not induce Cyp1a1 expression, but upregulate expression of Stc2. Hepatic Stc2 expression was shown to be reduced in both obese (ob/ob) and high-fat diet fed mice, and the

recombinant Stc2 administration downregulated expression of lipogenic genes and ameliorated hepatosteatosis (Jiao et al., 2017; Zhao et al., 2018). Therefore, it is conceivable that CA-induced AhR-mediated Stc2 upregulation activate anti-steatotic signaling to alleviate hepatic steatosis and inflammation *in vitro*. It is also plausible that other AhR target genes, cross-talking transcription factors, and signaling pathways including TLR4 (Liu et al., 2014), SREBP1 (Krishnan et al., 2018; Muku et al., 2019), estrogen signaling (Zhu et al., 2020), SOCS3 (Wada et al., 2016), NF- κ B (Larigot et al., 2018; Zeng et al., 2014) are involved in protection – albeit the exact mechanism of CA-mediated AhR-Stc2 dependent hepatoprotection *in vivo* is uncharacterized and future studies interrogating mechanism of protection against lipotoxicity are warranted.

The early stage of NAFLD is primarily characterized by excessive lipid accumulation in hepatocytes. This study was successful in mimicking the first stage of NAFLD pathology *in vitro* using palmitic acid and oleic acid (major FFAs found in NAFLD patients), and *in vivo* by feeding mice a high-fat diet (60 kcal%) – as evident by aggregation of large number of lipid droplets in hepatic cell lines (Fig. 1B), macrovascular steatosis in mice livers (Fig. 5A), and increase in triglyceride and cholesterol (Fig 5B-C). However, the treatment with CA significantly prevented the weight gain (Fig. 4A-C), attenuated steatosis (Fig. 1B and 5A), mitigated metabolic deterioration as see by lowered fasting glucose and improved glucose tolerance (Fig. 6), suppressed the inflammation due to high-fat diet feeding (Fig. 7E), and protected against hepatic injury (Fig. 5D). We identified that CA treatment downregulated expression of fatty acid translocase, CD36 (Fig. 3A) concomitantly with decrease in hepatic free fatty acid uptake (Fig. 2C). NAFLD patients have abnormally high levels of

CD36 that positively correlate with the histological grade of hepatic steatosis (Rada et al., 2020), whereas hepatocyte specific knockout of CD36 attenuated fatty liver disease and improved insulin sensitivity in high-fat diet fed mice (Wilson et al., 2016). Therefore, it is conceivable that CA regulates hepatic CD36 mediated uptake of long-chain fatty acids and alleviates hepatosteatosis. The reduced weight gain, without a change in food intake suggests that CA may act on other tissues in addition to the liver and that the reduction of CD36 may not be unique to the liver, therefore in future it will be important to determine whether CA alters adipose tissue thermogenesis and/or fatty acid uptake by gut (Rada et al., 2020). We did not observe significant changes in other fatty acid transporters including fatty acid transport protein 2 (FATP2) in response to CA treatment (data not shown). Both *in vitro* and *in vivo* studies showed that CA treatment after the onset of steatosis were able to mitigate metabolic deterioration and steatohepatitis. These data strongly suggest that the reversal of steatosis is not only by hindering lipogenesis but also via potential increase in the rate of mitochondrial fatty acid oxidation, and/or transport of triglycerides to other tissues including muscles and adipose. Accordingly, we identified elevation of rate-determining enzyme for mitochondrial beta-oxidation, CPT1a in response to CA treatment. However, marker of peroxisomal beta-oxidation ACOX1 was unaltered (Xu et al., 2021). Therefore, it is plausible that CA treatment preferentially activate hepatic mitochondrial oxidation and contribute in mitigating NAFLD, although whether CA stimulates SIRT1-PGC1 α signaling cascade needs to be determined. Further studies beyond the scope of this manuscript will also interrogate mechanism by which CA induced AhR-Stc2 signaling regulate specific lipid metabolism pathways and alleviate steatosis.

The findings of this study confirmed that CA bestowed hepatic protection in both *in vitro* and *in vivo* NAFLD models by suppressing hepatic free fatty acid uptake and regulating genes involved in lipid metabolism. CA improved glucose tolerance, dampened the expression of pro-inflammatory cytokines that exacerbate NAFLD pathology, and protected against hepatic steatosis and injury. Moreover, CA mediated hepatoprotection against fatty liver pathology was contingent upon AhR-mediated Stc2 expression. In summary, the identification of hepatoprotective function of endogenous AhR agonist, CA will be instrumental in the development of future novel therapeutic interventions against metabolic liver diseases.

AUTHORSHIP CONTRIBUTIONS

Participated in research design: Patil, Mandala, Friedman, Joshi

Conducted experiments: Patil, Rus, Downing

Contributed new reagents or analytic tools: Patil, Mandala

Performed data analysis: Patil, Joshi

Wrote or contributed to the writing of the manuscript: Patil, Rus, Downing, Friedman,
Mandala, Joshi

REFERENCES:

- Angulo P. (2002) Nonalcoholic fatty liver disease. *N Engl J Med* 346:1221-1231.
- Bugianesi E, Leone N, Vanni E, Marchesini G, Brunello F, Carucci P, Musso A, De Paolis P, Capussotti L, Salizzoni M. (2002) Expanding the natural history of nonalcoholic steatohepatitis: From cryptogenic cirrhosis to hepatocellular carcinoma. *Gastroenterology* 123:134-140.
- Carambia A and Schuran FA. (2021) The aryl hydrocarbon receptor in liver inflammation. *43:563-575*.
- Cobbina E and Akhlaghi F. (2017) Non-alcoholic fatty liver disease (NAFLD)–pathogenesis, classification, and effect on drug metabolizing enzymes and transporters. *Drug Metab Rev* 49:197-211.
- Cohen JC, Horton JD, Hobbs HH. (2011) Human fatty liver disease: Old questions and new insights. *Science* 332:1519-1523.
- Day CP and James OF. (1998) Steatohepatitis: A tale of two “hits”? *Gastroenterology* 114:842-845.
- de Alwis NMW and Day CP. (2008) Non-alcoholic fatty liver disease: The mist gradually clears. *J Hepatol* 48:S104-S112.

Denison MS and Nagy SR. (2003) Activation of the aryl hydrocarbon receptor by structurally diverse exogenous and endogenous chemicals. *Annu Rev Pharmacol Toxicol* 43:309-334.

Farrell GC and Larter CZ. (2006) Nonalcoholic fatty liver disease: From steatosis to cirrhosis. *Hepatology* 43:S99-S112.

Faul F, Erdfelder E, Buchner A, Lang A. (2009) Statistical power analyses using G* power 3.1: Tests for correlation and regression analyses. *Behavior Research Methods* 41:1149-1160.

Fazio F, Zappulla C, Notartomaso S, Busceti C, Bessede A, Scarselli P, Vacca C, Gargaro M, Volpi C, Allegrucci M. (2014) Cinnabarinic acid, an endogenous agonist of type-4 metabotropic glutamate receptor, suppresses experimental autoimmune encephalomyelitis in mice. *Neuropharmacology* 81:237-243.

Fernández T, Viñuela M, Vidal C, Barrera F. (2022) Lifestyle changes in patients with non-alcoholic fatty liver disease: A systematic review and meta-analysis. *PloS One* 17:e0263931.

Fernandez-Salguero PM, Pineau T, Hilbert DM, McPhail T, Lee SS, Kimura S, Nebert DW, Rudikoff S, Ward JM, Gonzalez FJ. (1995) Immune system impairment and hepatic fibrosis in mice lacking the dioxin – binding Ah receptor . *Science* 268:722-726.

Friedman SL, Neuschwander-Tetri BA, Rinella M, Sanyal AJ. (2018) Mechanisms of NAFLD development and therapeutic strategies. *Nat Med* 24:908-922.

Gómez-Piñeiro RJ, Dali M, Mansuy D, Boucher J. (2022) Unstability of cinnabarinic acid, an endogenous metabolite of tryptophan, under situations mimicking physiological conditions. *Biochimie* 199:150-157.

Guo L, Kang JS, Park YH, Je BI, Lee YJ, Kang NJ, Park SY, Hwang DY, Choi YW. (2020) S-petasin inhibits lipid accumulation in oleic acid-induced HepG2 cells through activation of the AMPK signaling pathway. *Food & Function* 11:5664-5673.

Harper TA, Joshi AD, Elferink CJ. (2013) Identification of stanniocalcin 2 as a novel aryl hydrocarbon receptor target gene. *J Pharmacol Exp Ther* 344:579-588.

Hendrikx T and Schnabl B. (2019) Indoles: Metabolites produced by intestinal bacteria capable of controlling liver disease manifestation. *J Intern Med* 286:32-40.

Ipsen DH, Lykkesfeldt J, Tveden-Nyborg P. (2018) Molecular mechanisms of hepatic lipid accumulation in non-alcoholic fatty liver disease. *Cellular and Molecular Life Sciences* 75:3313-3327.

Ji Y, Gao Y, Chen H, Yin Y, Zhang W. (2019) Indole-3-acetic acid alleviates nonalcoholic fatty liver disease in mice via attenuation of hepatic lipogenesis, and oxidative and inflammatory stress. *Nutrients* 11:2062.

Jiao Y, Zhao J, Shi G, Liu X, Xiong X, Li X, Zhang H, Ma Q, Lu Y. (2017) Stanniocalcin2 acts as an anorectic factor through activation of STAT3 pathway. *Oncotarget* 8:91067.

Joshi AD, Thinakaran G, Elferink C. (2022) Cinnabarinic acid-induced stanniocalcin 2 confers cytoprotection against alcohol-induced liver injury. *J Pharmacol Exp Ther* 381:1-11.

Joshi AD. (2020) New insights into physiological and pathophysiological functions of stanniocalcin 2. *Frontiers in Endocrinology* 11:172.

Joshi AD, Carter DE, Harper TA, Elferink CJ. (2015) Aryl hydrocarbon receptor-dependent stanniocalcin 2 induction by cinnabarinic acid provides cytoprotection against endoplasmic reticulum and oxidative stress. *J Pharmacol Exp Ther* 353:201-212.

Kawano Y and Cohen DE. (2013) Mechanisms of hepatic triglyceride accumulation in non-alcoholic fatty liver disease. *J Gastroenterol* 48:434-441.

Krishnan S, Ding Y, Saedi N, Choi M, Sridharan GV, Sherr DH, Yarmush ML, Alaniz RC, Jayaraman A, Lee K. (2018) Gut microbiota-derived tryptophan metabolites modulate inflammatory response in hepatocytes and macrophages. *Cell Reports* 23:1099-1111.

Larigot L, Juricek L, Dairou J, Coumoul X. (2018) AhR signaling pathways and regulatory functions. *Biochimie Open* 7:1-9.

Le MH, Yeo YH, Li X, Li J, Zou B, Wu Y, Ye Q, Huang DQ, Zhao C, Zhang J, Liu C, Chang N, Xing F, Yan S, Wan ZH, Tang NSY, Mayumi M, Liu X, Liu C, Rui F, Yang H, Yang Y, Jin R, Le RHX, Xu Y, Le DM, Barnett S, Stave CD, Cheung R, Zhu Q, Nguyen

MH. (2021) 2019 global NAFLD prevalence: A systematic review and meta-analysis. *Clinical Gastroenterology and Hepatology* .

Lee JH, Wada T, Febbraio M, He J, Matsubara T, Lee MJ, Gonzalez FJ, Xie W. (2010) A novel role for the dioxin receptor in fatty acid metabolism and hepatic steatosis. *Gastroenterology* 139:653-663.

Liu Y, She W, Wang F, Li J, Wang J, Jiang W. (2014) 3, 3'-diindolylmethane alleviates steatosis and the progression of NASH partly through shifting the imbalance of treg/Th17 cells to treg dominance. *Int Immunopharmacol* 23:489-498.

Lowe MM, Mold JE, Kanwar B, Huang Y, Louie A, Pollastri MP, Wang C, Patel G, Franks DG, Schlezinger J. (2014) Identification of cinnabarinic acid as a novel endogenous aryl hydrocarbon receptor ligand that drives IL-22 production. *PloS One* 9:e87877.

Ma C, Marlowe JL, Puga A. (2009) The aryl hydrocarbon receptor at the crossroads of multiple signaling pathways. *Molecular, Clinical and Environmental Toxicology* :231-257.

Ma Q. (2001) Induction of CYP1A1. the AhR/DRE paradigm transcription, receptor regulation, and expanding biological roles. *Curr Drug Metab* 2:149-164.

Michel MC, Murphy T, Motulsky HJ. (2020) New author guidelines for displaying data and reporting data analysis and statistical methods in experimental biology. *J Pharmacol Exp Ther* 372:136-147.

Mimura J and Fujii-Kuriyama Y. (2003) Functional role of AhR in the expression of toxic effects by TCDD. *Biochimica Et Biophysica Acta (BBA)-General Subjects* 1619:263-268.

Mitchell KA, Lockhart CA, Huang G, Elferink CJ. (2006) Sustained aryl hydrocarbon receptor activity attenuates liver regeneration. *Mol Pharmacol* 70:163-170.

Muku GE, Blazanin N, Dong F, Smith PB, Thiboutot D, Gowda K, Amin S, Murray IA, Perdew GH. (2019) Selective ah receptor ligands mediate enhanced SREBP1 proteolysis to restrict lipogenesis in sebocytes. *Toxicological Sciences* 171:146-158.

Murray IA and Perdew GH. (2020) How ah receptor ligand specificity became important in understanding its physiological function. *International Journal of Molecular Sciences* 21:9614.

Nault R, Fader KA, Ammendolia DA, Dornbos P, Potter D, Sharratt B, Kumagai K, Harkema JR, Lunt SY, Matthews J. (2016) Dose-dependent metabolic reprogramming and differential gene expression in TCDD-elicited hepatic fibrosis. *Toxicological Sciences* 154:253-266.

Nebert DW, Puga A, Vasiliou V. (1993) Role of the ah receptor and the dioxin-inducible [ah] gene battery in toxicity, cancer, and signal transduction. *Ann N Y Acad Sci* 685:624-640.

Ochi T, Kawaguchi T, Nakahara T, Ono M, Noguchi S, Koshiyama Y, Munekage K, Murakami E, Hiramatsu A, Ogasawara M. (2017) Differences in characteristics of

glucose intolerance between patients with NAFLD and chronic hepatitis C as determined by CGMS. *Scientific Reports* 7:1-9.

Park KT, Mitchell KA, Huang G, Elferink CJ. (2005) The aryl hydrocarbon receptor predisposes hepatocytes to fas-mediated apoptosis. *Mol Pharmacol* 67:612-622.

Patil NY, Tang H, Rus I, Zhang K, Joshi AD. (2022) Decoding cinnabarinic Acid-Specific stanniocalcin 2 induction by aryl hydrocarbon receptor. *Mol Pharmacol* 101:45-55.

Pierre S, Chevallier A, Teixeira-Clerc F, Ambolet-Camoit A, Bui L, Bats A, Fournet J, Fernandez-Salguero P, Aggerbeck M, Lotersztajn S. (2014) Aryl hydrocarbon receptor-dependent induction of liver fibrosis by dioxin. *Toxicological Sciences* 137:114-124.

Postic C and Girard J. (2008) The role of the lipogenic pathway in the development of hepatic steatosis. *Diabetes Metab* 34:643-648.

Probst MR, Reisz-Porszasz S, Agbunag RV, Ong MS, Hankinson O. (1993) Role of the aryl hydrocarbon receptor nuclear translocator protein in aryl hydrocarbon (dioxin) receptor action. *Mol Pharmacol* 44:511-518.

Rada P, González-Rodríguez Á, García-Monzón C, Valverde ÁM. (2020) Understanding lipotoxicity in NAFLD pathogenesis: Is CD36 a key driver? *Cell Death & Disease* 11:1-15.

Reyes H, Reisz-Porszasz S, Hankinson O. (1992) Identification of the ah receptor nuclear translocator protein (arnt) as a component of the DNA binding form of the ah receptor. *Science* 256:1193-1195.

Safe S, Han H, Goldsby J, Mohankumar K, Chapkin RS. (2018) Aryl hydrocarbon receptor (AhR) ligands as selective AhR modulators: Genomic studies. *Current Opinion in Toxicology* 11:10-20.

Savouret J, Berdeaux A, Casper R. (2003) The aryl hydrocarbon receptor and its xenobiotic ligands: A fundamental trigger for cardiovascular diseases. *Nutrition, Metabolism and Cardiovascular Diseases* 13:104-113.

Shetty A and Syn W. (2019) Health and economic burden of nonalcoholic fatty liver disease in the united states and its impact on veterans. *Federal Practitioner* 36:14.

Tilg H and Moschen AR. (2010) Evolution of inflammation in nonalcoholic fatty liver disease: The multiple parallel hits hypothesis. *Hepatology* 52:1836-1846.

Wada T, Sunaga H, Miyata K, Shirasaki H, Uchiyama Y, Shimba S. (2016) Aryl hydrocarbon receptor plays protective roles against high fat diet (HFD)-induced hepatic steatosis and the subsequent lipotoxicity via direct transcriptional regulation of Socs3 gene expression. *J Biol Chem* 291:7004-7016.

Walisser JA, Glover E, Pande K, Liss AL, Bradfield CA. (2005) Aryl hydrocarbon receptor-dependent liver development and hepatotoxicity are mediated by different cell types. *Proceedings of the National Academy of Sciences* 102:17858-17863.

White DL, Kanwal F, El-Serag HB. (2012) Association between nonalcoholic fatty liver disease and risk for hepatocellular cancer, based on systematic review. *Clinical Gastroenterology and Hepatology* 10:1342-1359. e2.

Wilson CG, Tran JL, Erion DM, Vera NB, Febbraio M, Weiss EJ. (2016) Hepatocyte-specific disruption of CD36 attenuates fatty liver and improves insulin sensitivity in HFD-fed mice. *Endocrinology* 157:570-585.

Wójcik-Cichy K, Koślińska-Berkan E, Piekarska A. (2018) The influence of NAFLD on the risk of atherosclerosis and cardiovascular diseases. *Clinical and Experimental Hepatology* 4:1.

Wright EJ, De Castro KP, Joshi AD, Elferink CJ. (2017) Canonical and non-canonical aryl hydrocarbon receptor signaling pathways. *Current Opinion in Toxicology* 2:87-92.

Wu R, Zhang L, Hoagland MS, Swanson HI. (2007) Lack of the aryl hydrocarbon receptor leads to impaired activation of AKT/protein kinase B and enhanced sensitivity to apoptosis induced via the intrinsic pathway. *J Pharmacol Exp Ther* 320:448-457.

Xia H, Zhu X, Zhang X, Jiang H, Li B, Wang Z, Li D, Jin Y. (2019) Alpha-naphthoflavone attenuates non-alcoholic fatty liver disease in oleic acid-treated HepG2 hepatocytes and in high fat diet-fed mice. *Biomedicine & Pharmacotherapy* 118:109287.

Xu N, Luo H, Li M, Wu J, Wu X, Chen L, Gan Y, Guan F, Li M, Su Z. (2021) B-patchoulene improves lipid metabolism to alleviate non-alcoholic fatty liver disease via activating AMPK signaling pathway. *Biomedicine & Pharmacotherapy* 134:111104.

Zeng L, Tang WJ, Yin JJ, Zhou BJ. (2014) Signal transductions and nonalcoholic fatty liver: A mini-review. *Int J Clin Exp Med* 7:1624-1631.

Zhang C and Yang M. (2021) Current options and future directions for NAFLD and NASH treatment. *International Journal of Molecular Sciences* 22:7571.

Zhao J, Jiao Y, Song Y, Liu J, Li X, Zhang H, Yang J, Lu Y. (2018) Stanniocalcin 2 ameliorates hepatosteatosis through activation of STAT3 signaling. *Frontiers in Physiology* 9:873.

Zhou H, Wu H, Liao C, Diao X, Zhen J, Chen L, Xue Q. (2010) Toxicology mechanism of the persistent organic pollutants (POPs) in fish through AhR pathway. *Toxicology Mechanisms and Methods* 20:279-286.

Zhu X, Xia H, Wang Z, Li B, Jiang H, Li D, Jin R, Jin Y. (2020) In vitro and in vivo approaches for identifying the role of aryl hydrocarbon receptor in the development of nonalcoholic fatty liver disease. *Toxicol Lett* 319:85-94.

FOOTNOTES

This work was supported by the National Institute of Diabetes and Digestive and Kidney Diseases grant R01-DK122028, and Presbyterian Health Foundation – Harold Hamm Diabetes Center Seed Grant (to A. D. J.); and R01-DK121951 (to J. E. F.). Authors report no conflict of interest.

FIGURE LEGENDS

Fig. 1. Determination of (A) cell viability of HepG2 cells treated with different concentrations of palmitic acid (PA) and oleic acid (OA) for 24 hrs. Cell viability was measured by a luminescent assay and expressed relative to BSA-treated control. Data are represented as mean \pm SD (n=3). *p<0.05 compared to control group. (B) CA protects against palmitic acid (PA)/oleic acid (OA)-induced steatosis. Representative images of oil red O stained HepG2 cells treated with 500 μ M BSA + DMSO (control), 30 μ M CA, 500 μ M PA, 500 μ M OA, 30 μ M CA+ 500 μ M PA/OA, 30 μ M CA after 500 μ M PA/OA. (C) Quantification of oil red O-stained images; area of oil red O stained lipid droplets was normalized to the total area (3 images per treatment) and (D) quantification of accumulated oil red O by colorimetry; absorbance measured at 500 nm. Data are represented as mean \pm SD (n=3). *p<0.05 compared to PA/OA-only treatment group.

Fig. 2. Quantification of (A) triglyceride, (B) free fatty acid content and (C) free fatty acid uptake in HepG2 cells treated with 500 μ M BSA + DMSO (control), 30 μ M CA, 500 μ M PA, 500 μ M OA, 30 μ M CA+ 500 μ M PA/OA, 30 μ M CA after 500 μ M PA/OA. Triglyceride content was measured using luminescence assay, whereas free fatty acid content and free fatty acid uptake was determined fluorometrically. Data are represented as mean \pm SD (n=3). *p<0.05 compared to PA/OA-only treatment group.

Fig. 3. Expression of mRNAs encoding genes involved in (A) free fatty acid transport, (B) fatty acid synthesis, (C) triglyceride synthesis, and (D) inflammation. HepG2 cells

were treated with 500 μ M BSA+ DMSO (control), 30 μ M CA, 500 μ M PA, 500 μ M OA, 30 μ M CA+ 500 μ M PA/OA, 30 μ M CA after 500 μ M PA/OA. mRNA message was analyzed by qRT-PCR and normalized to 18S rRNA. Results are expressed as fold of the value found in control treatment arbitrarily set at 1. For statistical analysis, a mixed-effects multivariate ANOVA (MANOVA) model was used. After an overall significant F test from MANOVA model, the post hoc multiple-comparison tests were performed for the pre-specified comparisons adjusted by Tukey procedure. Data are represented as mean \pm SD (n=3). *p<0.05 compared to PA/OA-only treatment group.

Fig. 4. CA treatment reduces body and liver weight of high fat diet-fed mice. C57BL6 mice were fed with control diet (CD) for 16 weeks, high fat diet (HFD) for 16 weeks, high-fat diet and treated with CA for 16 weeks (CA + HFD), and high-fat diet for 16 weeks with CA treatment initiated after 10 weeks of exposure to HFD for remaining 6 weeks (CA after HFD). (A) Representative image of mice after 16 weeks of diet, (B) body mass, (C) body weight at the end of the study, week 16, (D) weight of the liver at week 16, (E) percentage ratio of liver weight normalized to total body weight at the end of the study, and (F) daily food intake calculated from the average of weekly food intake. Data are represented as mean \pm SD (n=7). *p<0.05 compared to HFD-only treatment group.

Fig. 5. CA alleviates steatosis and hepatic injury in high fat diet-fed mice. (A) Representative image of H&E-stained liver sections, (B) liver triglycerides, (C) liver cholesterol, and (D) serum ALT measurement of mice fed with control diet (CD) for 16

weeks, high fat diet (HFD) for 16 weeks, high-fat diet and treated with CA for 16 weeks (CA + HFD), and high-fat diet for 16 weeks with CA treatment initiated after 10 weeks of exposure to HFD for remaining 6 weeks (CA after HFD). Data are represented as mean \pm SD (n=7). *p<0.05 compared to HFD-only treatment group.

Fig. 6. CA lowers blood glucose levels and improves glucose tolerance in HFD-fed mice. Mice were fed with control diet (CD), high fat diet (HFD) , high-fat diet with CA treatment (CA + HFD) for 16 weeks, and with high-fat diet for 16 weeks with CA treatment initiated after 10 weeks of HFD feeding for the last 6 weeks (CA after HFD). (A) fasting blood glucose measurement, (B) glucose tolerance test performed, and (C) the area under the curve calculated for respective groups. Data are represented as mean \pm SD (n=7). *p<0.05 compared to HFD-only treatment group.

Fig. 7. CA attenuates hepatic free fatty acid uptake, lipogenesis and inflammation *in vivo*. C57BL6 mice were fed with control diet (CD) for 16 weeks, high fat diet (HFD) for 16 weeks, high-fat diet and CA treatment for 16 weeks (CA + HFD), and high-fat diet for 16 weeks with CA treatment for last 6 weeks (CA after HFD). mRNA expression of markers for (A) free fatty acid transport, (B) *de novo* lipogenesis, (C) triglyceride synthesis, (D) fatty acid oxidation, and (E) inflammation were analyzed by qRT-PCR and normalized to 18S rRNA. Results are expressed as fold of the value found in control treatment arbitrarily set at 1. Data are represented as mean \pm SD (n=7). *p<0.05 compared to HFD-only treatment group.

Fig. 8. CA failed to protect against NAFLD in an AhR-silenced *in vitro* model. HepG2 cells were transiently transfected with AhR or non-targeting (scrambled) siRNA for 24 hrs followed by 500 μ M BSA+ DMSO (control), 30 μ M CA, 500 μ M PA, 500 μ M OA, 30 μ M CA+ 500 μ M PA, 30 μ M CA+ 500 μ M OA and/or 30 μ M CA 24 hrs after 500 μ M PA/OA treatments. (A) Western blotting on total lysate was performed to monitor AhR expression. Actin was probed as a control, (B) Oil red O staining to detect lipid content. Quantification of (C) triglyceride, (D) free fatty acid content, and (E) free fatty acid uptake; mRNA expression of genes involved in (F) free fatty acid uptake, (G) fatty acid synthesis, (H) triglyceride synthesis, and (I) inflammation, normalized to 18S rRNA. Data are represented as mean \pm SD (n=3). *p<0.05 compared to untransfected control group not treated with CA.

Fig. 9. CA mediated protection against lipotoxicity is Stc2 dependent. HepG2 cells were transiently transfected with Stc2 or non-targeting (scrambled) siRNA for 24 hrs. followed by 500 μ M BSA+ DMSO (control), 30 μ M CA, 500 μ M PA, 500 μ M OA, 30 μ M CA+ 500 μ M PA, 30 μ M CA+ 500 μ M OA and/or 30 μ M CA 24 hrs after 500 μ M PA/OA treatments. (A) Stc2 expression in total lysate was monitored by performing immunoblotting. Actin was used as a control, (B) Lipid content was detected using oil red O staining. Quantification of (C) triglyceride, (D) free fatty acid, and (E) free fatty acid uptake. Expression of genes involved in (F) free fatty acid uptake, (G) fatty acid synthesis, (H) triglyceride synthesis, and (I) inflammation, was quantitated by performing quantitative RT-PCR, normalized to 18S rRNA. Data are represented as mean \pm SD (n=3). *p<0.05 compared to untransfected control group untreated with CA.

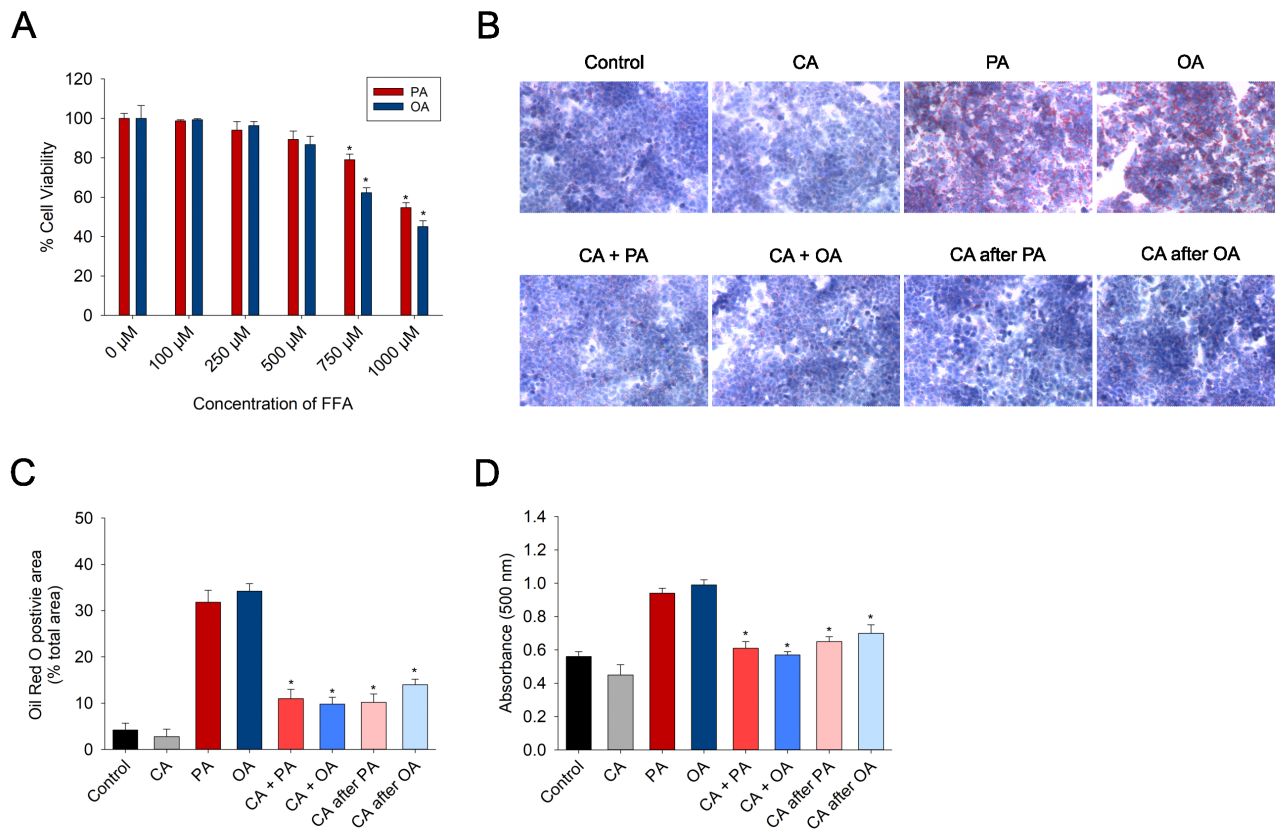


Figure 1

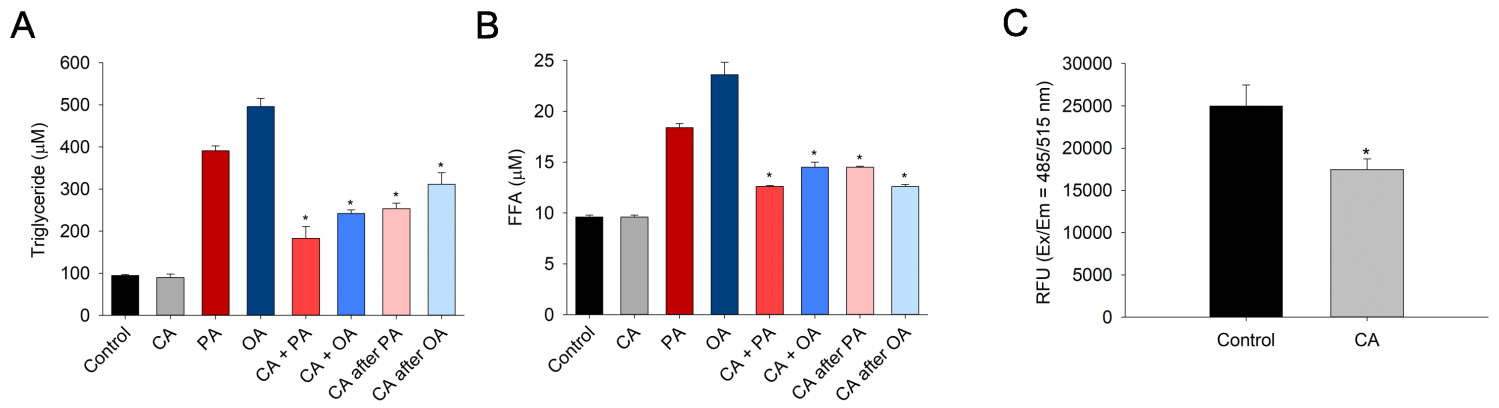


Figure 2

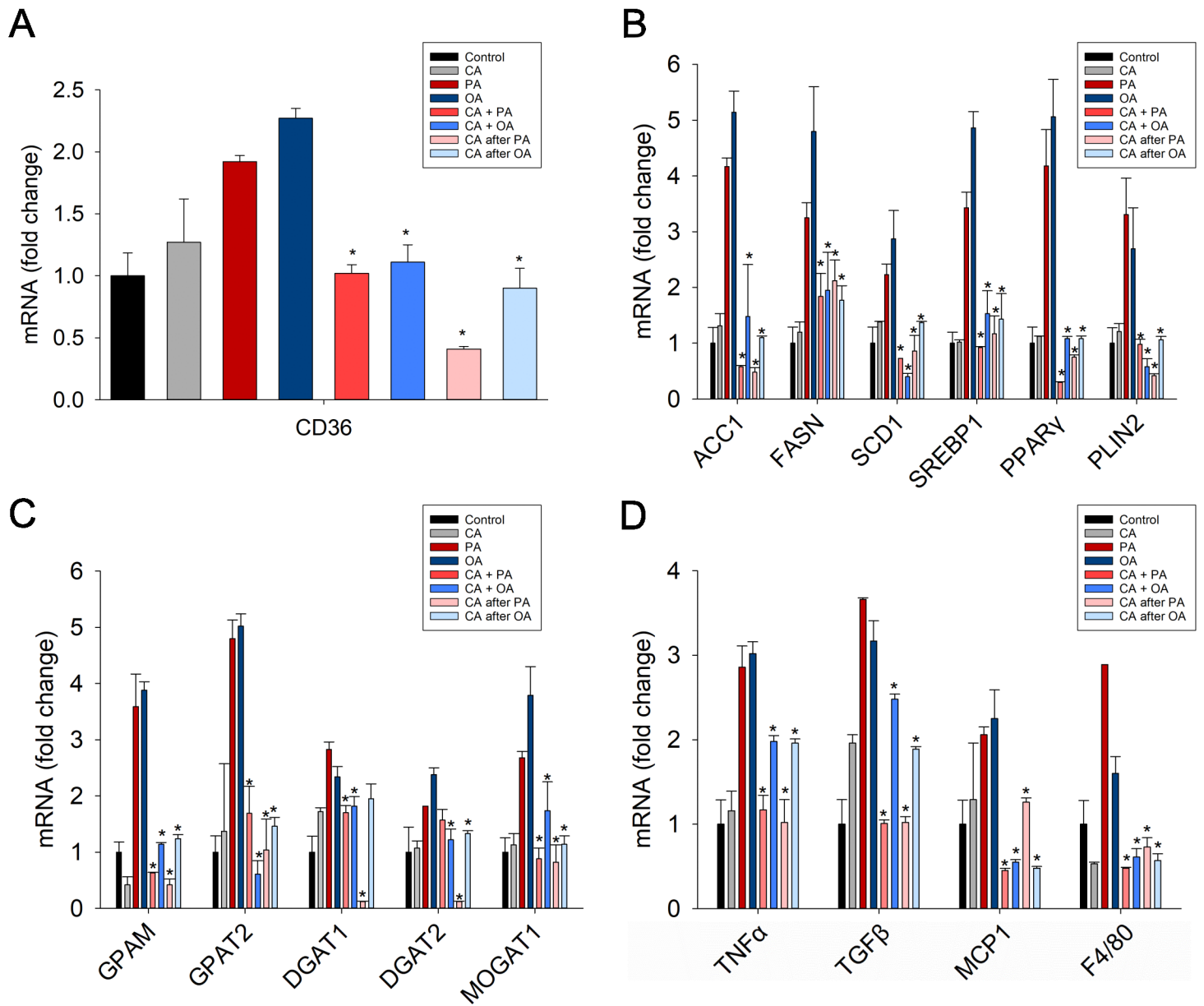


Figure 3

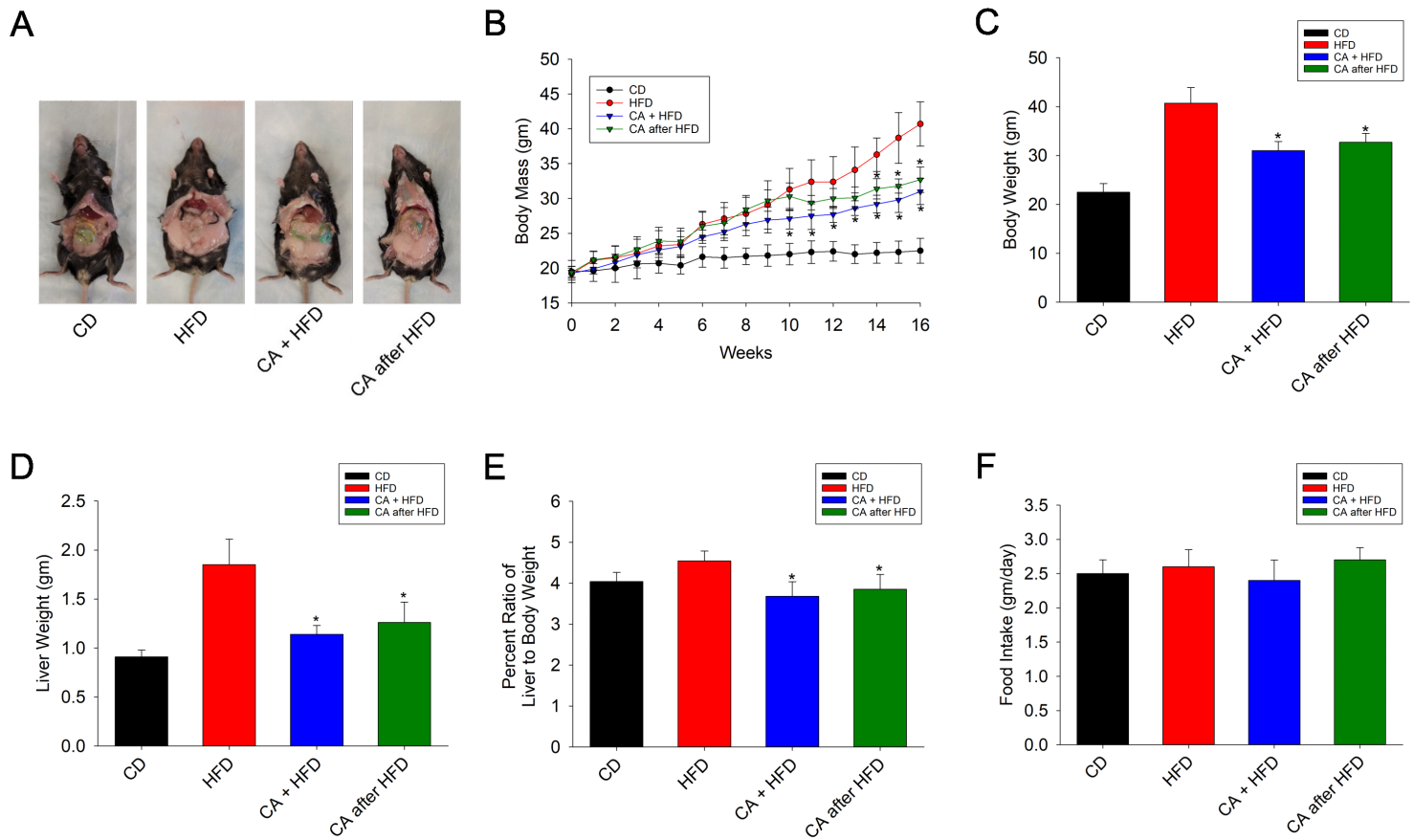


Figure 4

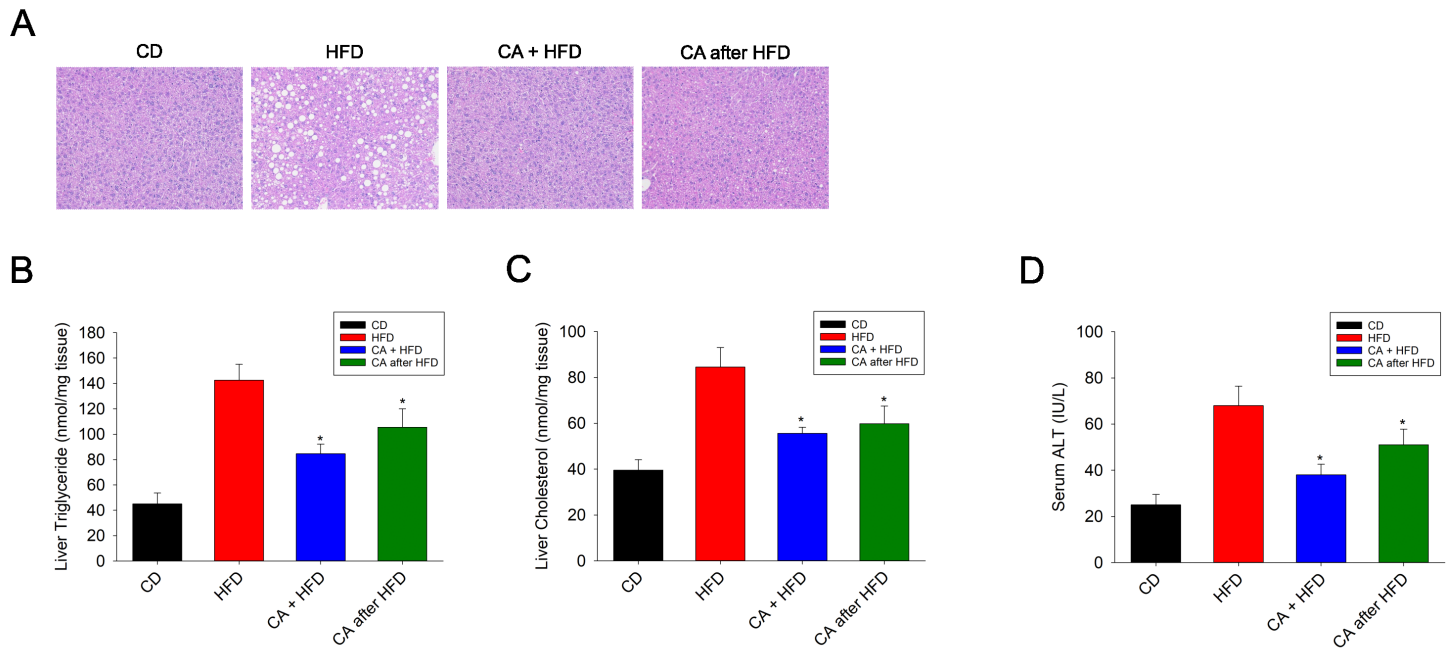


Figure 5

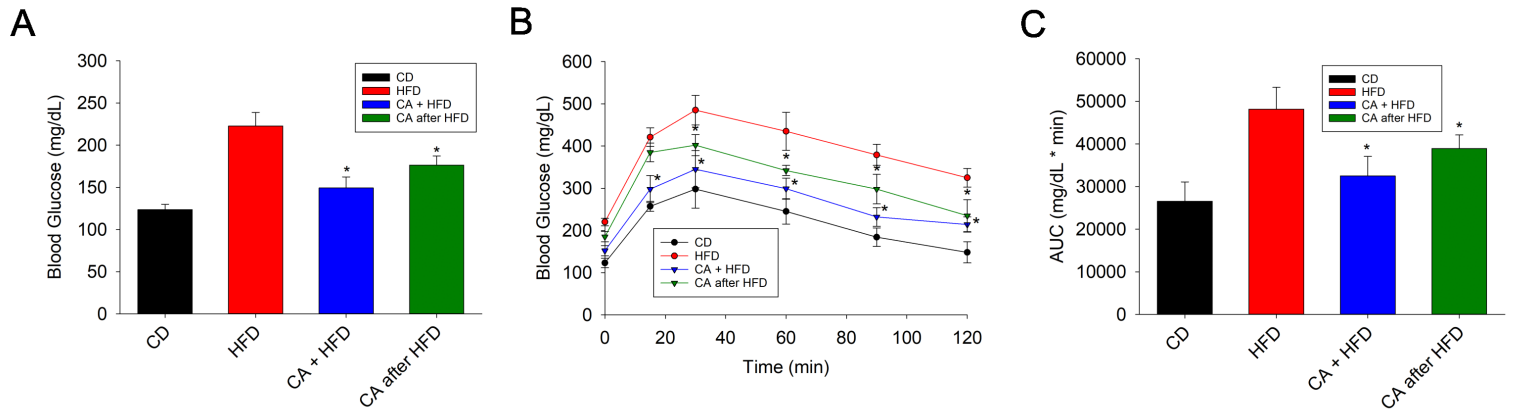


Figure 6

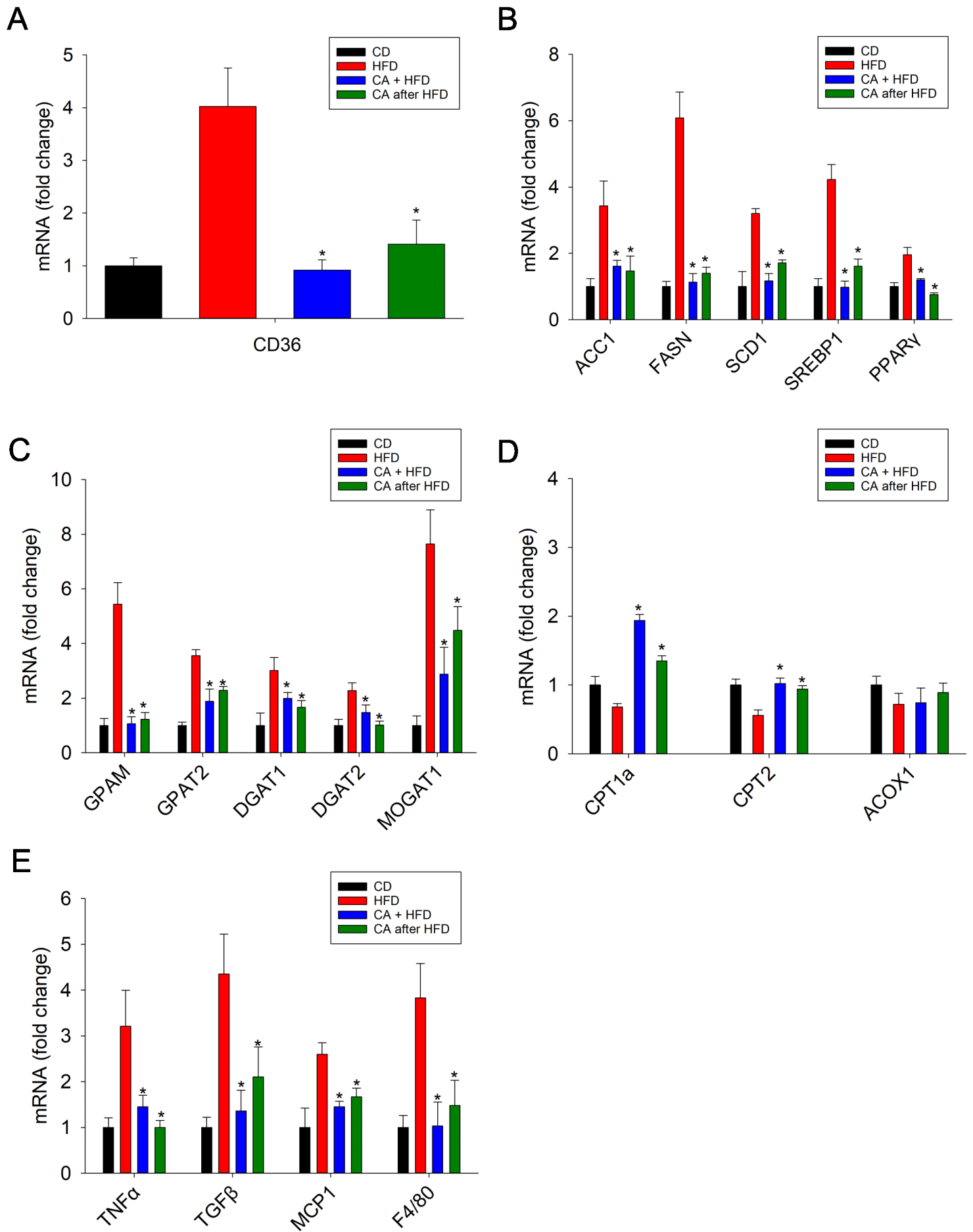


Figure 7

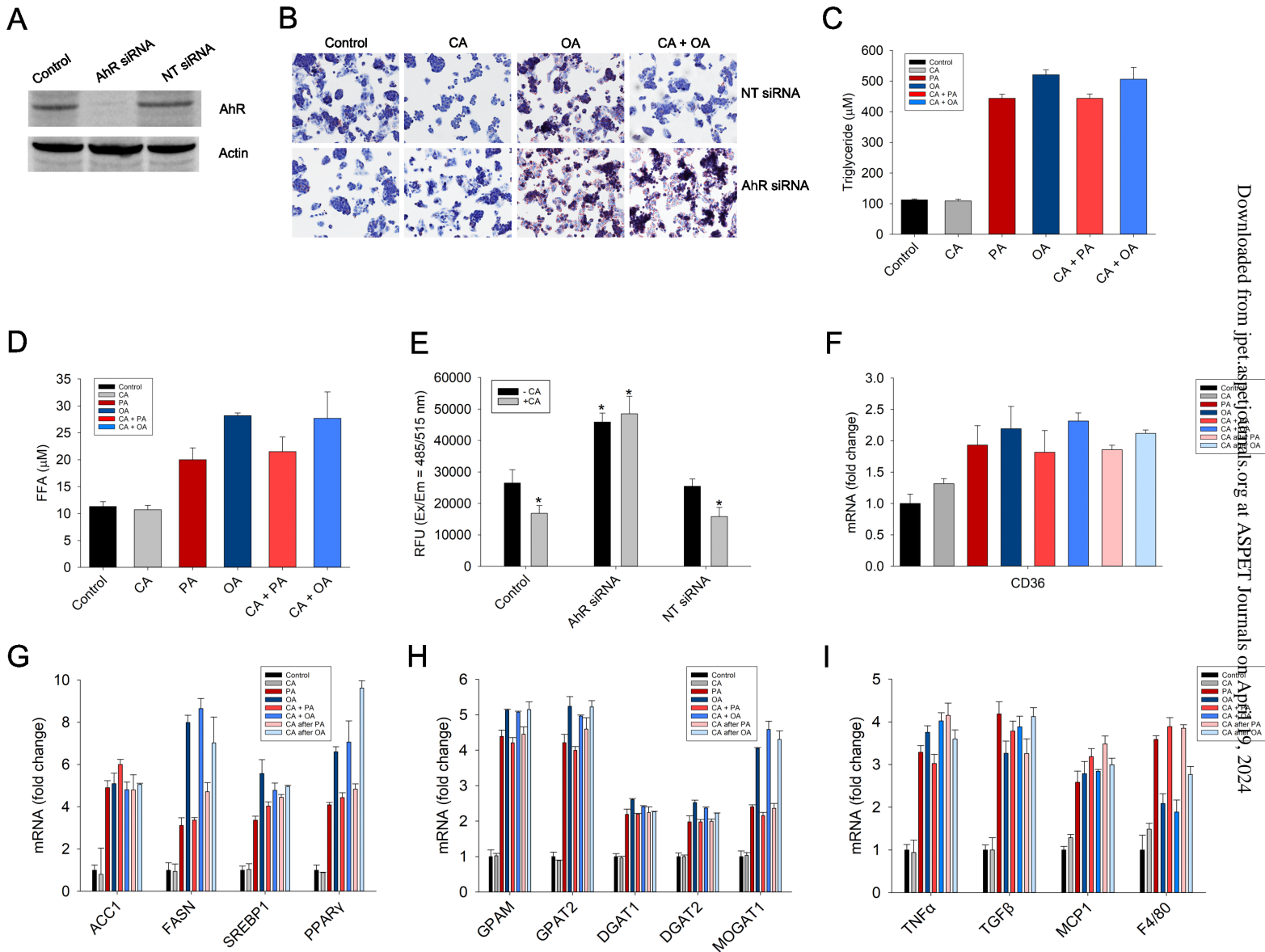


Figure 8

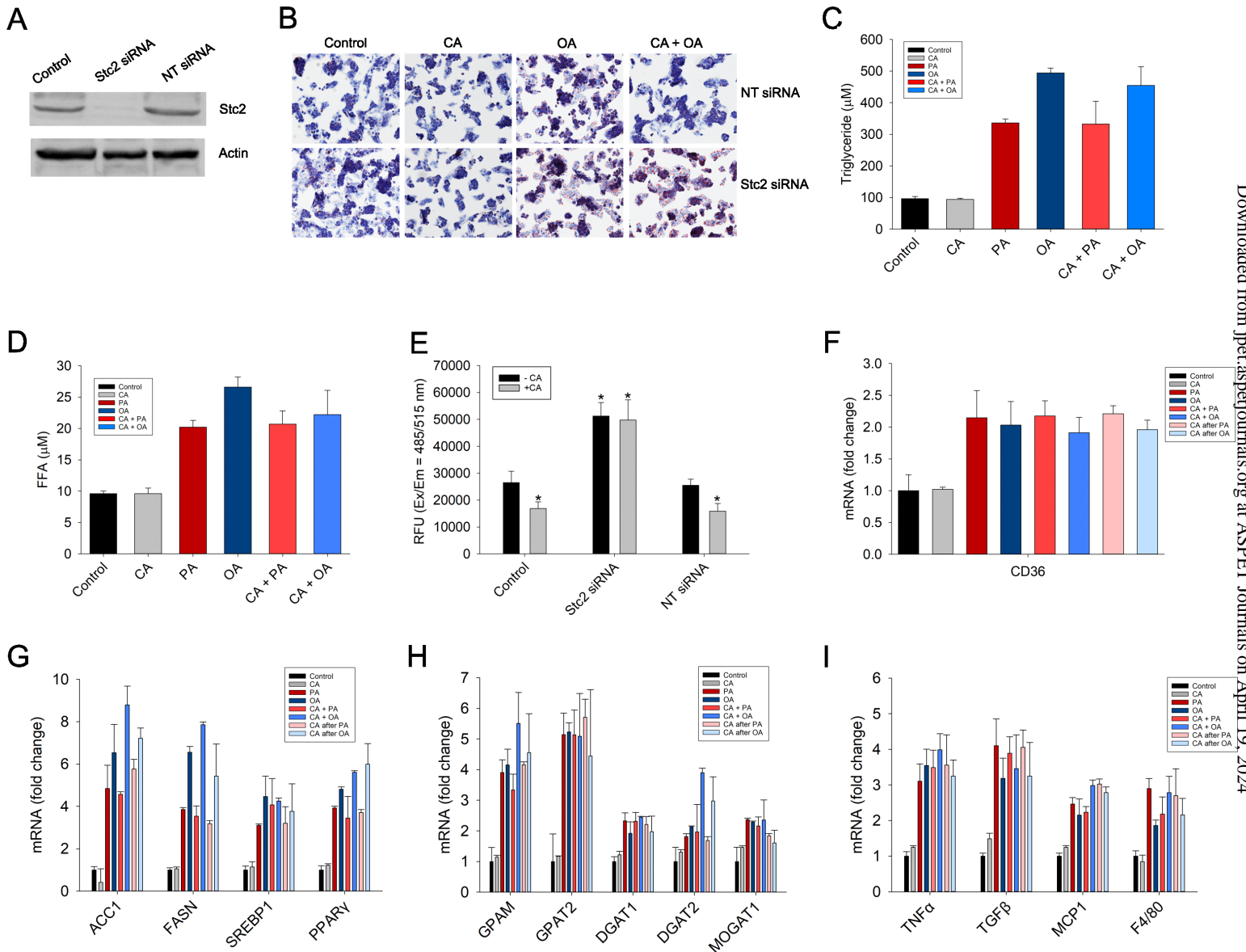


Figure 9